


See discussions, stats, and author profiles for this publication at: <https://www.researchgate.net/publication/233741124>

A Study on Corrosion Durability of Ferrocement


Article in *ACI Materials Journal* · January 2008


CITATIONS
2

3 authors, including:


 **M. Maalqj**
University of Sharjah
70 PUBLICATIONS 1,629 CITATIONS
[SEE PROFILE](#)

Some of the authors of this publication are also working on these related projects:

 Green Drivers Behaviour [View project](#)

 Experimental study on shear strength of trapezoidal corrugated steel webs [View project](#)

READS
169

 **Mohammad Ismail**
Universiti Teknologi Malaysia
84 PUBLICATIONS 274 CITATIONS
[SEE PROFILE](#)



VOL. 105, NO. 1
JANUARY-FEBRUARY 2008

DR. MOHAMMAD ISMAIL
Profesor Madya
Jabatan Struktur & Bahan
Fakulti Kejuruteraan Awam
Universiti Teknologi Malaysia

MATERIALS JOURNAL

- 3 Prediction of Reinforcement Corrosion in Concrete and Its Effects on Concrete Cracking and Strength Reduction/*C.-Q. Li, Y. Yang, and R. E. Melchers*
- 11 Bond Properties of High-Strength Carbon Fiber-Reinforced Polymer Strands/*W. Xue, X. Wang, and S. Zhang*
- 20 Effectiveness of Alkyl Alkoxy Silane Treatment in Mitigating Alkali-Silica Reaction/*K. Tosun, B. Felekoglu, and B. Baradan*
- 28 Study on Corrosion Durability of Ferrocement/*M. A. Mansur, M. Maalej, and M. Ismail*
- 35 Salt Weathering Distress on Concrete Exposed to Sodium Sulfate Environment/*H. Haynes, R. O'Neill, M. Neff, and P. K. Mehta*
- 44 Validation of Mualem's Conductivity Model and Prediction of Saturated Permeability from Sorptivity/*C. Leech, D. Lockington, R. D. Hooton, G. Galloway, G. Cowin, and P. Dux*
- 52 Heat Loss Compensation in Semi-Adiabatic Curing Test of Concrete/*P. L. Ng, I. Y. T. Ng, and A. K. H. Kwan*
- 62 Experimental Asymptotic Analysis of Expansion of Concrete Exposed to Sulfate Attack/*P. J. M. Monteiro and K. E. Kurtis*
- 72 Performance of Two Anchor Systems of Externally Bonded Fiber-Reinforced Polymer Laminates/*N. Eshwar, A. Nanni, and T. J. Ibell*
- 81 Full-Scale Marine Exposure Tests on Treated and Untreated Concretes—Initial 7-Year Results/*S. V. Nanukuttan, L. Basheer, W. J. McCarter, D. J. Robinson, and P. A. M. Basheer*
- 88 Use of Thixotropy-Enhancing Agent to Reduce Formwork Pressure Exerted by Self-Consolidating Concrete/*K. H. Khayat and J. J. Assaad*
- 97 Experimental Simulation of Self-Consolidating Concrete Formwork Pressure/*A. Gregori, R. P. Ferron, Z. Sun, and S. P. Shah*

A JOURNAL OF THE AMERICAN CONCRETE INSTITUTE



American Concrete Institute®
Advancing concrete knowledge

Board of Direction

President

David Darwin

Vice Presidents

Florian G. Barth
Luis E. García

Directors

Sergio M. Alcocer
Kenneth B. Bondy
Ramón L. Carrasquillo
S. K. Ghosh
Charles S. Hanskat
Richard E. Klingner
Jon I. Mullarky
Myles A. Murray
Julio A. Ramirez
Michael J. Schneider
Eldon G. Tipping
Kari L. Yuers

Past President Board Members

Anthony E. Fiorato
James R. Cagley
Thomas D. Verti

Executive Vice President

William R. Tolley

Technical Activities Committee

Ronald G. Burg, Chair
Daniel W. Falconer, Secretary
Kenneth B. Bondy
Ronald Janowiak
Claude E. Jaycox
David W. Johnston
Steven H. Kosmatka
Michael E. Kreger
David A. Lange
James E. McDonald
Myles A. Murray
Hani H. Nassif
David H. Sanders
Charles A. Zalesiak

Staff

Executive Vice President
William R. Tolley

Publishing Services

Supervisor
John Q. Horn

Editors
Carl R. Bischof
Emily H. Bush
Karen Czedik

Production Assistant
Lindsay K. Kennedy

Manuscript Review Coordinator
Jamie A. McMann

Administrative Assistant
Daniela A. Bedward

Engineering

Managing Director
Daniel W. Falconer

Chief Engineer
Shuaib H. Ahmad

Staff Engineers
Matthew R. Senecal
Miroslav F. Vejvoda

ACI Materials Journal

JANUARY-FEBRUARY 2008, VOL. 105, NO. 1

A JOURNAL OF THE AMERICAN CONCRETE INSTITUTE
AN INTERNATIONAL TECHNICAL SOCIETY

- 3 Prediction of Reinforcement Corrosion in Concrete and Its Effects on Concrete Cracking and Strength Reduction**, by Chun-Qing Li, Yang Yang, and Robert E. Melchers
- 11 Bond Properties of High-Strength Carbon Fiber-Reinforced Polymer Strands**, by Weichen Xue, Xiaohui Wang, and Shulu Zhang
- 20 Effectiveness of Alkyl Alkoxy Silane Treatment in Mitigating Alkali-Silica Reaction**, by Kamile Tosun, Burak Felekoglu, and Bülent Baradan
- 28 Study on Corrosion Durability of Ferrocement**, by M. A. Mansur, Mohamed Maalej, and Mohammad Ismail
- 35 Salt Weathering Distress on Concrete Exposed to Sodium Sulfate Environment**, by Harvey Haynes, Robert O'Neill, Michael Neff, and P. Kumar Mehta
- 44 Validation of Mualem's Conductivity Model and Prediction of Saturated Permeability from Sorptivity**, by Craig Leech, David Lockington, R. Doug Hooton, Graham Galloway, Gary Cowin, and Peter Dux
- 52 Heat Loss Compensation in Semi-Adiabatic Curing Test of Concrete**, by P. L. Ng, I. Y. T. Ng, and A. K. H. Kwan
- 62 Experimental Asymptotic Analysis of Expansion of Concrete Exposed to Sulfate Attack**, by Paulo J. M. Monteiro and Kimberly E. Kurtis
- 72 Performance of Two Anchor Systems of Externally Bonded Fiber-Reinforced Polymer Laminates**, by Nagaraj Eshwar, Antonio Nanni, and Timothy James Ibell
- 81 Full-Scale Marine Exposure Tests on Treated and Untreated Concretes—Initial 7-Year Results**, by Sreejith V. Nanukuttan, Lulu Basheer, W. John McCarter, Des J. Robinson, and P. A. Muhammed Basheer
- 88 Use of Thixotropy-Enhancing Agent to Reduce Formwork Pressure Exerted by Self-Consolidating Concrete**, by Kamal H. Khayat and Joseph J. Assaad
- 97 Experimental Simulation of Self-Consolidating Concrete Formwork Pressure**, by Amedeo Gregori, Raissa P. Ferron, Zhihui Sun, and Surendra P. Shah
- 105 In ACI Structural Journal**

Discussion is welcomed for all materials published in this issue and will appear in the November-December 2008 issue if received by August 1, 2008. Discussion of material received after specified dates will be considered individually for publication or private response.

ACI Standards published in ACI Journals for public comment have discussion due dates printed with the Standard.

Annual index published in the March-April issue.

ACI Materials Journal

Copyright © 2008 American Concrete Institute. Printed in the United States of America.

The *ACI Materials Journal* (ISSN 0889-325x) is published bimonthly by the American Concrete Institute. Publication office: 38800 Country Club Drive, Farmington Hills, MI 48331. Periodicals postage paid at Farmington, MI, and at additional mailing offices. Subscription rates: \$155 per year (U.S. and possessions), \$163 (elsewhere), payable in advance. POSTMASTER: Send address changes to: *ACI Materials Journal*, P. O. Box 9094, Farmington Hills, MI 48333-9094.

Canadian GST: R 1226213149.

Direct correspondence to P.O. Box 9094, Farmington Hills, MI 48333-9094. Telephone: (248) 848-3700. Facsimile (FAX): (248) 848-3701. Website: <http://www.concrete.org>.

DR. MOHAMMAD ISMAIL

Profesor Madya

Jabatan Struktur & Bahan

Title no. 105-M04

Study on Corrosion Durability of Ferrocement

by M. A. Mansur, Mohamed Maalej, and Mohammad Ismail

An electrochemical-based accelerated corrosion technique has been employed to study the corrosion durability of ferrocement. Variables considered include cover thickness; composition of the matrix in terms of water-cement ratio (w/c), sand-cement ratio (s/c), and contents of mineral and chemical admixtures; and use of stainless steel wire mesh. After suitable exposure, maximum crack width, percentage of steel loss, and reduction in flexural strength served as the bases for assessing the relative performance of various means considered.

Test results indicate that the addition of mineral admixtures, application of a suitable surface coating, and the use of deeper concrete cover provide excellent protection against reinforcement corrosion. Employment of stainless steel as reinforcement and the use of so-called corrosion inhibitor or a low w/c in the matrix also slows down the corrosion process, but is not as effective as others. Based on test results, a hybrid protection system combining three lines of defense is suggested for enhanced durability of ferrocement.

Keywords: corrosion; cracking; ductility; durability; ferrocement; protective system; strength; tests.

INTRODUCTION

Thin-walled cement composites, such as ferrocement and other laminated composites, are being increasingly used in many applications where a strong and tough protective shell is needed in both new and existing structures.^{1,2} But because of a very thin cover to the reinforcement, as small as 3 mm (0.12 in.), the long-term durability of these composites is being frequently questioned. No satisfactory answer to this vital question exists because of the lack of adequate research information. A recent case study³ has revealed that, despite the use of traditional galvanized wire mesh, significant corrosion damage could occur within a decade of natural exposure if no additional measures are undertaken. The current awareness of the importance of durability has been reflected in a survey conducted by RILEM Committee 48-FC⁴ on existing ferrocement structures. Also, in its recently formulated model code,⁵ the International Ferrocement Society has identified this area where available information is insufficient to make any general recommendations. This has hindered the growth and general acceptability of this otherwise attractive material in structural applications.

Although considerable literature⁶⁻⁸ does exist on the topic of corrosion of steel reinforcement in conventional concrete, there seems to be a general reluctance in applying the overall findings with confidence to thin-walled cement composites because of some fundamental differences between the two materials. In contrast to conventional reinforced concrete, the overall thickness of ferrocement and other laminated composites rarely exceeds 25 mm (1 in.), the reinforcing elements are distributed evenly and dispersed more uniformly (large specific surface) with a very thin concrete protection, and coarse aggregates are removed from the matrix. Due to these differences, the mechanics of the corrosion process and its outcome may differ considerably. Hence,

there is an urgent need to address the question of durability as affected by corrosion of steel reinforcement in thin-walled composites and to find ways to enhance its long-term performance.

The possible solution to the potential corrosion problem by preventing or delaying/slowing down the process would obviously lie in the three lines of defense—protective coating on the reinforcing element itself, the quality of the matrix that surrounds it, and the surface coatings of the overall composite. Keeping this strategy in view, the present research program has been directed toward finding a suitable protective system by evaluating each measure separately for the three lines of defense of the system. Because natural corrosion of steel embedded in a cement-based matrix takes decades to cause significant damage, an accelerated corrosion technique comprising the galvanostatic method and cyclic wetting and drying in a sodium chloride solution has been employed. After a predetermined period of exposure, maximum width of cracks, steel losses, and degradation of flexural strength have been determined to assess the extent of corrosion damage or, in other words, establish the effectiveness of the protective measure. Based on the analysis and evaluation of observed performances, recommendations are made for a suitable hybrid protection system for enhanced durability of ferrocement.

RESEARCH SIGNIFICANCE

A proper assessment of the corrosion problems in thin-walled cement-based composites and finding a suitable protective system, at least to delay the corrosion process either by modifying the matrix and its composition or by applying some suitable coating to the reinforcement and/or to the surface of the composite, will undoubtedly have a great impact in the construction industry. In addition to having a durable material suitable for numerous applications, ferrocement could be a material of choice for the enormous repair and rehabilitation industry offering cost-effective solutions to many problems.

EXPERIMENTAL INVESTIGATION

Test program

The present experimental program has been designed to establish a suitable protective system against reinforcement corrosion in thin-walled ferrocement structures. Three lines of defense—protection of reinforcement by surface coating (type of steel) and matrix cover, quality and constituents of the matrix, and overall surface coating—have been considered separately. The protective measures or parameters considered

ACI Materials Journal, V. 105, No. 1, January-February 2008.

MS No. M-2006-406 received October 9, 2006, and reviewed under Institute publication policies. Copyright © 2008, American Concrete Institute. All rights reserved, including the making of copies unless permission is obtained from the copyright proprietors. Pertinent discussion including authors' closure, if any, will be published in the November-December 2008 *ACI Materials Journal* if the discussion is received by August 1, 2008.

M. A. Mansur is a Professor of civil engineering at the Universiti Teknologi Malaysia, Johor Darul Takzim, Malaysia. He received the ACI Maurice P. Van Buren Structural Engineering Award (now the ACI Design Award) in 1989 and 1992. He received his engineering degrees from Bangladesh University of Engineering and Technology, Dhaka, Bangladesh, and his PhD from the University of New South Wales, Sydney, Australia. His research interests include reinforced structural concrete, fiber reinforcement in concrete, and ferrocement.

Mohamed Maalej is an Associate Professor in the Department of Civil and Environmental Engineering at the University of Sharjah, Sharjah, UAE. He received his MEng from Massachusetts Institute of Technology, Cambridge, MA, and a PhD from the University of Michigan, Ann Arbor, MI. His research interests include micromechanics-based design of fiber-reinforced cementitious composites for infrastructural applications, impact/blast resistance of engineered cementitious composites, and corrosion durability of reinforced concrete.

Mohammad Ismail is an Associate Professor and Head of the Department of Structures and Materials, Faculty of Civil Engineering, Universiti Teknologi Malaysia. He received his BScEng from the University of Strathclyde, Glasgow, Scotland; his MScEng from the University of Liverpool, Liverpool, UK; and his PhD from the University of Aston, Birmingham, UK. His research interests include corrosion of reinforcement in concrete, structural assessment and structural health monitoring using advanced technologies, and structural repair and strengthening.

in this study, together with the details of the test program, are presented in Table 1. Table 2 furnishes detailed compositions of various mortar mixtures employed.

A total of 65 specimens, divided into 13 groups, were prepared. Each group consisted of five identical specimens to investigate a particular parameter. Among them, two were kept under natural environment and the remaining three were

Table 1—Test program

Type of protection	Test parameter	Description	Specimen group	Mortar mixture designation
Reference*			Control	CM
Direct protection to steel	Corrosion inhibitor	Prescribed dose	CI	CM+
	Concrete cover, mm (in.)	3 (0.12)	CC-3	CM
		6 (0.24)	CC-6	CM
Quality of matrix	w/c	0.35	w/c-0.35	w/c-0.35
		0.50	w/c-0.50	w/c-0.50
	s/c	1.5	s/c-1.5	s/c-1.5
		2.5	s/c-2.5	s/c-2.5
	Fly ash/cement	25%	FA-25	FA-25
		50%	FA-50	FA-50
Silica fume/cement	10%	SF-10	SF-10	
Surface protection	Surface coating	Elastomeric paint	SC	CM

*Concrete cover = 5 mm (0.2 in.); w/c = 0.43; s/c = 2.0; no admixture; and no surface coating.

Table 2—Details of mortar mixtures

Details		Mortar mixture								
		CM	WC-0.35	WC-0.50	SC-1.5	SC-2.5	FA-25	FA-50	SF-10	CM+
Constituents	Cement, kg/m ³	661	695	630	757	586	661	661	661	661
	Water (kg/m ³)	281	243	315	332	249	281	281	281	281
	Sand (kg/m ³)	1322	1391	1259	1136	1466	1322	1322	1322	1322
	Fly ash (kg/m ³)	—	—	—	—	—	165	330	—	—
	Silica fume (kg/m ³)	—	—	—	—	—	—	—	66	—
	Corrosion inhibitor (L/m ³)	—	—	—	—	—	—	—	—	5.0
w/c		0.43	0.35	0.50	0.43	0.43	0.43	0.43	0.43	0.43
s/c		2.0	2.0	2.0	1.5	2.5	2.0	2.0	2.0	2.0
Compressive strength, MPa (ksi)		59 (8.56)	64.7 (9.38)	59.4 (8.61)	73.9 (10.72)	58.5 (8.48)	61.9 (8.98)	53.9 (7.82)	85.2 (12.35)	78.1 (11.32)

Note: 1 kg/m³ = 1.68 lb/yd³; 1 L/m³ = 1.01 gal./yd³.

exposed to an accelerated corrosion regime by impressing a current to the embedded reinforcement and subjecting the specimens to cyclic wetting and drying using a sodium chloride solution. The effectiveness of a particular parameter/method in delaying and/or slowing the corrosion process was then evaluated using the maximum crack width, loss of steel, and deterioration of flexural strength resulting from corrosion of embedded reinforcement as the assessment criteria.

Test specimens

The dimensions of test specimens and the arrangement of reinforcement are shown in Fig. 1. Table 1 summarizes the test program. All specimens were identical as far as the overall dimensions and the amount of reinforcement were concerned. They were 330 mm (13 in.) long, 100 mm (4 in.) wide, and 20 mm (0.79 in.) thick, and each contained four layers of welded wire mesh of 12.7 mm (0.5 in.) square grid and 1 mm (0.04 in.) wire diameter as reinforcement. Similar to traditional ferrocement, galvanized meshes with a yield strength $f_y = 432$ MPa (62.6 ksi) and a modulus of elasticity $E_s = 200$ GPa (29,000 ksi) were used in all specimens, except for those in Group SS which had stainless steel meshes with $f_y = 460$ MPa (66.7 ksi) and $E_s = 200$ GPa (29,000 ksi). The mesh pieces were bundled in pairs and arranged symmetrically in the section, as shown in Fig. 1, leaving the desired clear cover of 5 mm (0.2 in.), except for specimens in Groups CC-3 and CC-6, where the cover was 3 mm (0.12 in.) and 6 mm (0.24 in.), respectively, on either side. All four mesh pieces were subsequently soldered together at one end for electrical

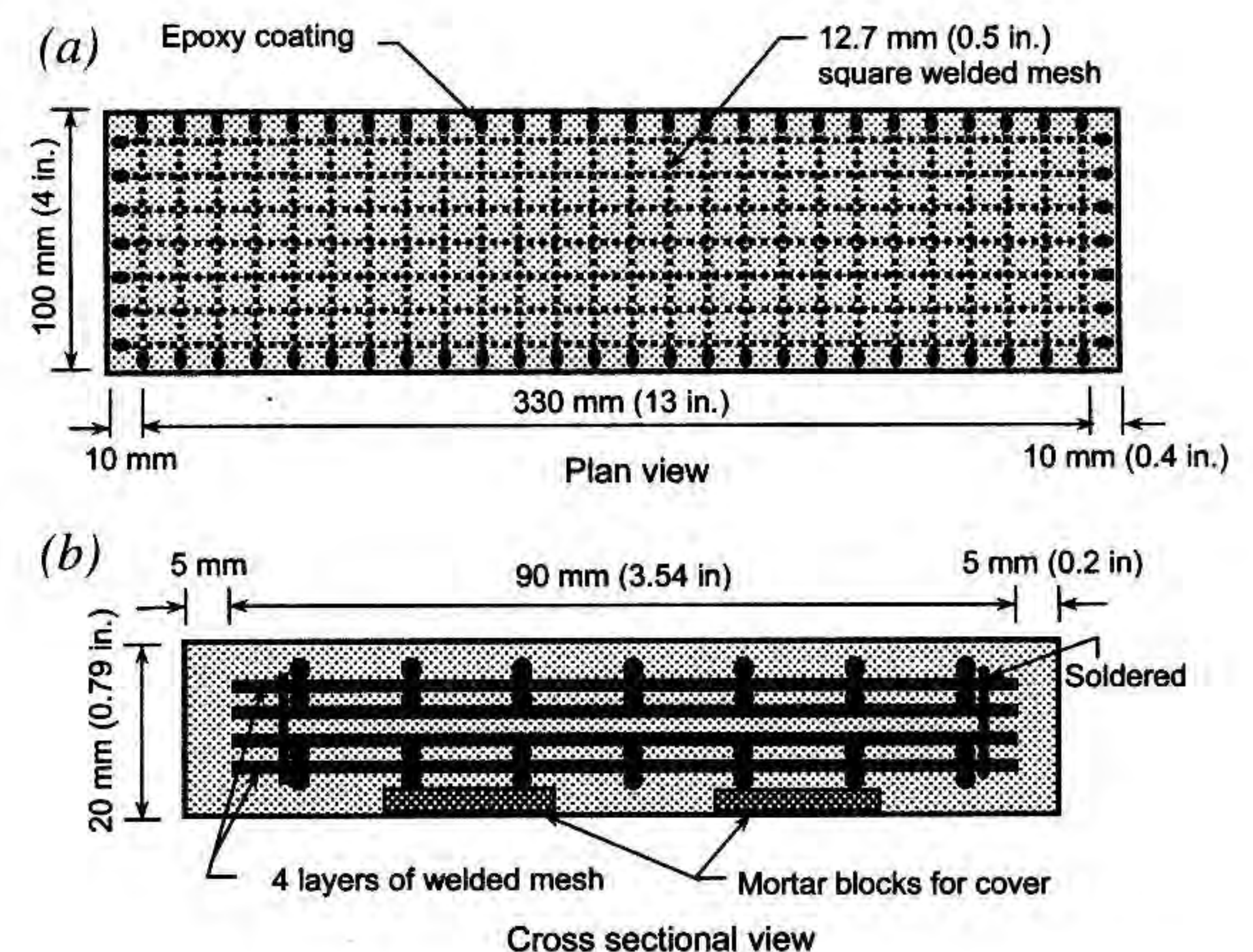


Fig. 1—Dimensions and reinforcement details of test specimens.

connection and the cut edges of the mesh layers were coated with epoxy resin to prevent early initiation of corrosion.

Ordinary portland cement and natural river sand passing through No. 8 sieve (2.36 mm or 0.09 in.) were used in the ratio of 1:2 for the control mortar, designated as CM (refer to Table 1). The water-cement ratio (w/c) for this mixture was 0.425. Fly ash and silica fume used in other mixtures (refer to Table 2) were obtained from local sources. The corrosion inhibiting admixture used in Mixture CI was obtained locally from an international construction chemical company based in Singapore. It is claimed that the use of this organic-based admixture in concrete forms a strong and durable film on the reinforcing steel, thus slowing the ingress of chlorides and extending the service life of the structure. For the specimen group designated SC in Table 1, an elastomeric coating based on acrylic copolymer, obtained from the same source as the corrosion-inhibiting admixture, was used as surface coating.

For each mortar mixture, the required ingredients were blended in a rotary mixer. Casting of the specimens was done on a vibrating table together with at least three 100 mm (4 in.) cubes for each mixture. The molds were removed the next day and both the test and control specimens were then cured in a fog room for 21 days before air-drying in the laboratory. The average 28-day cube compressive strengths of mortar for various mixtures are presented in Table 2.

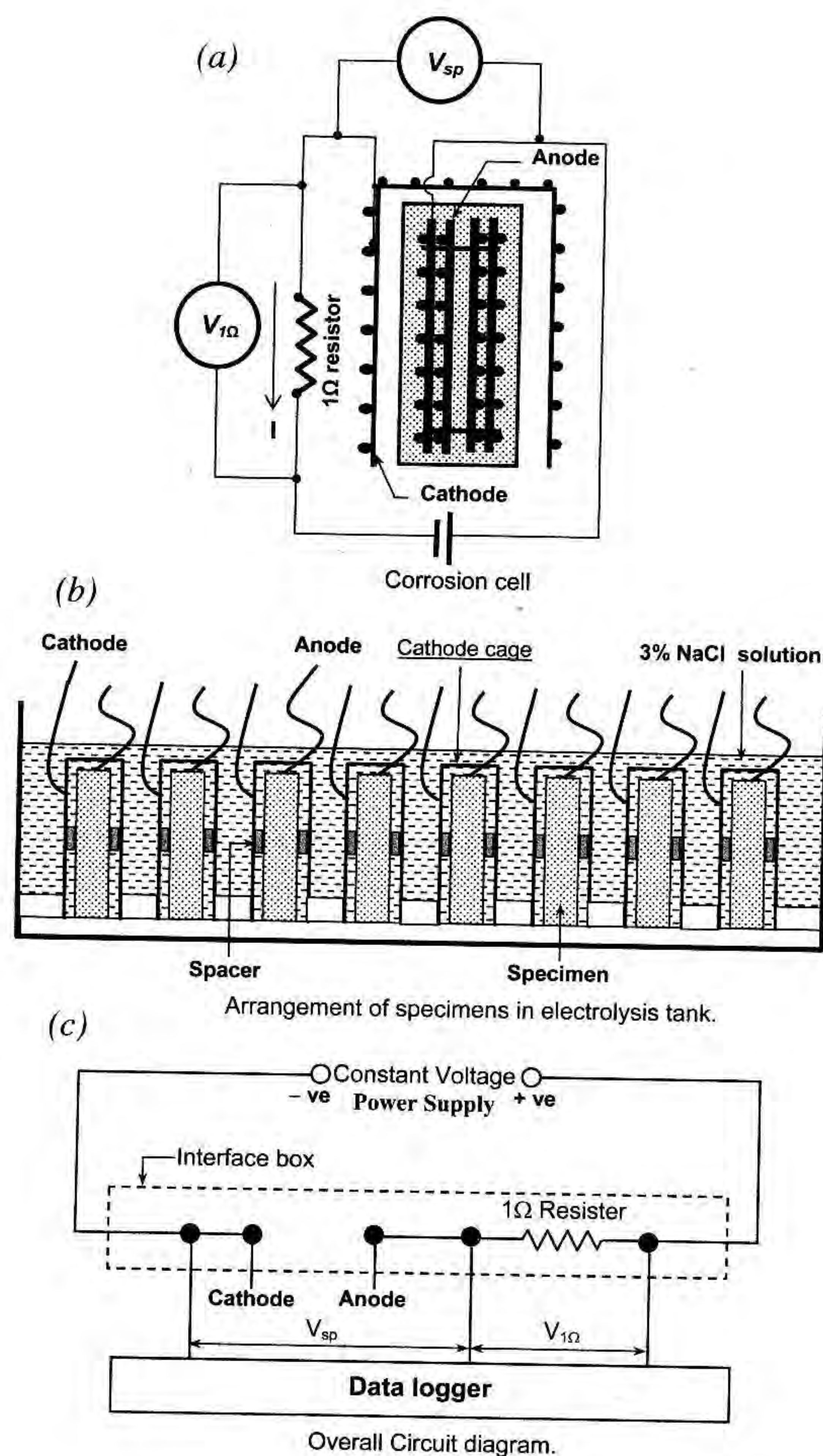


Fig. 2—Schematic of setup for accelerated corrosion tests using constant potential.

Test setup

The test specimens were subjected to an accelerated corrosion process using a galvanostatic method in which a current was impressed through the reinforcement by applying a fixed potential across the anode (internal reinforcement) and an external cathode wrapped around the specimen. The cathode was made out of the same wire mesh having approximately the same surface area as the anode to ensure a balance of free ion flow during the exposure regime. A schematic diagram of the corrosion cell for each specimen is illustrated in Fig. 2(a).

Five special tanks (glass fiber-reinforced polymer) were fabricated to hold the specimens in an upright position. A plastic rack with 35 mm (1.4 in.) spacers was placed in each tank to separate the specimens to avoid contact of cathode cages of adjacent specimens. Each tank could accommodate a maximum of eight specimens. The arrangement of specimens in the electrolysis tank is shown in Fig. 2(b).

The specimens were first connected in parallel using an interface box. The circuit was formed by connecting the anode and cathode terminals through a 1-Ohm resistor to the power supply. The power supply had dual channels—each capable of delivering a maximum of 12 volts with 10-ampere current. The complete circuit diagram for the galvanostatic method is shown in Fig. 2(c).

Test procedure

Once the circuit for the constant potential setup was ready, the tank was filled with 3% sodium chloride solution, and the circuit was activated. The initial voltage across the 1-Ohm resistor was recorded for each specimen. In this case, the current flowing through the specimens was effectively equivalent to the voltage measured in accordance with Ohm's Law because the register had a resistance of 1 Ohm. Next, the currents flowing through the specimens were adjusted such that all of them were subjected to the same initial magnitude of corrosion current. The specimens were then allowed to corrode and current readings were automatically recorded on an hourly interval using a data acquisition system.

To accelerate the corrosion process, the specimens were subjected to cyclic wetting and drying using a 3% (by weight) sodium chloride solution. Each cycle consisted of 1 day of wet phase and 2-1/2 days of dry phase, as suggested by Lee.⁹ During the wet phase, the specimens were fully immersed in the solution and, for the dry cycle, the solution was pumped out to below the base level of the specimens. The specimens were inspected visually for the initiation of any cracks at the end of each dry cycle. On the 30th day of exposure, the specimens were removed from the tank and the cracks, if any, were marked. Before commencing the next wet cycle, the solution was checked and the sodium chloride replenished whenever necessary. An overall view of the setup for accelerated corrosion tests displaying wet and dry cycles is shown in Fig. 3.

The accelerated corrosion regime was terminated on the 58th day when significant corrosion damage had occurred. The specimens were then recovered from the tank, allowed to dry, visible cracks were marked, and the maximum width of the cracks was measured using a hand-held microscope with an accuracy of ± 0.01 mm (0.004 in.). These corroded specimens, together with those left under the natural laboratory environment, were subsequently tested in flexure with the mold face down under third-point loading (refer to Fig. 4) to

evaluate any loss of strength and changes in the overall response as a result of corrosion of embedded steel reinforcement.

TEST RESULTS AND DISCUSSION

The principal test results generated from this program are summarized in Table 3. These include information on cracking (initiation and propagation of cracks and maximum crack width), continuous monitoring of corrosion currents translated subsequently into steel loss, and degradation of flexural strength as a result of corrosion of reinforcing steel.

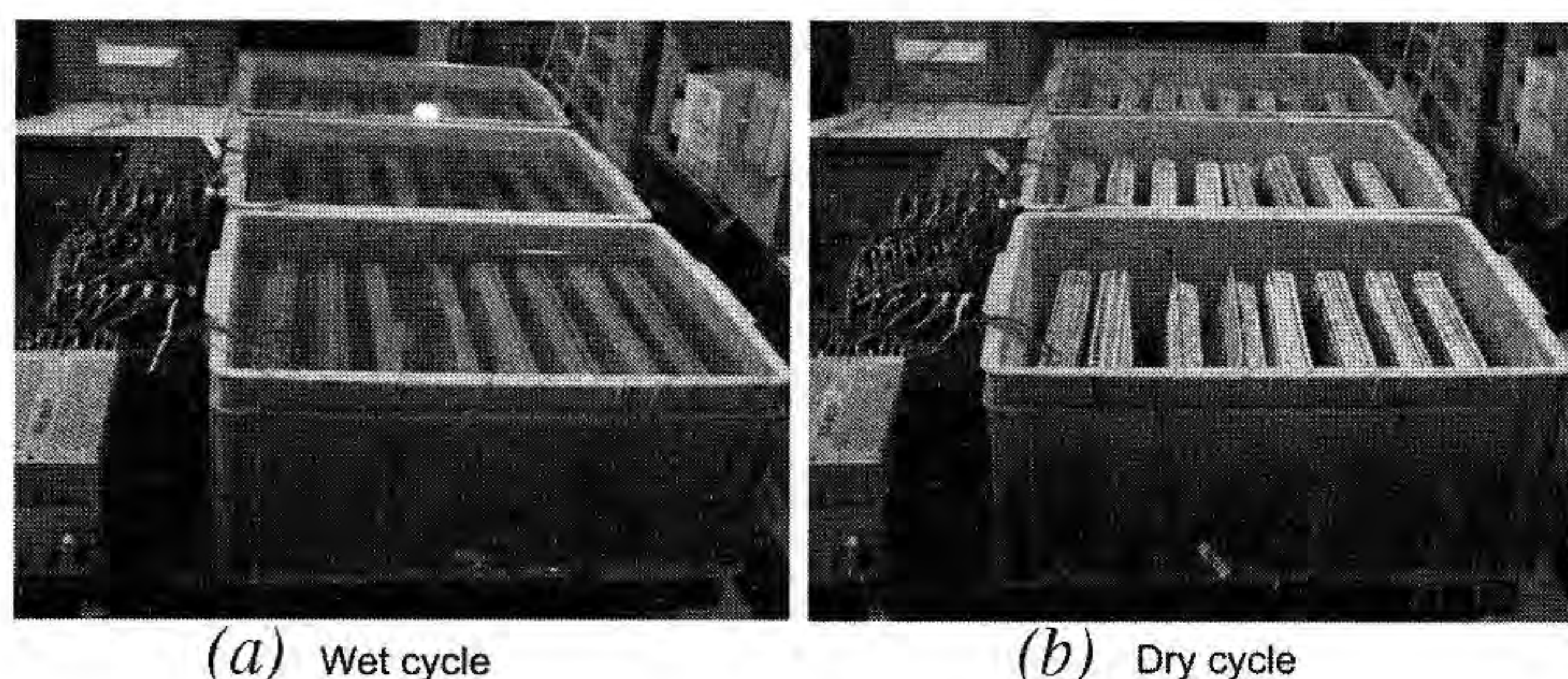


Fig. 3—View of setup for accelerated corrosion test.

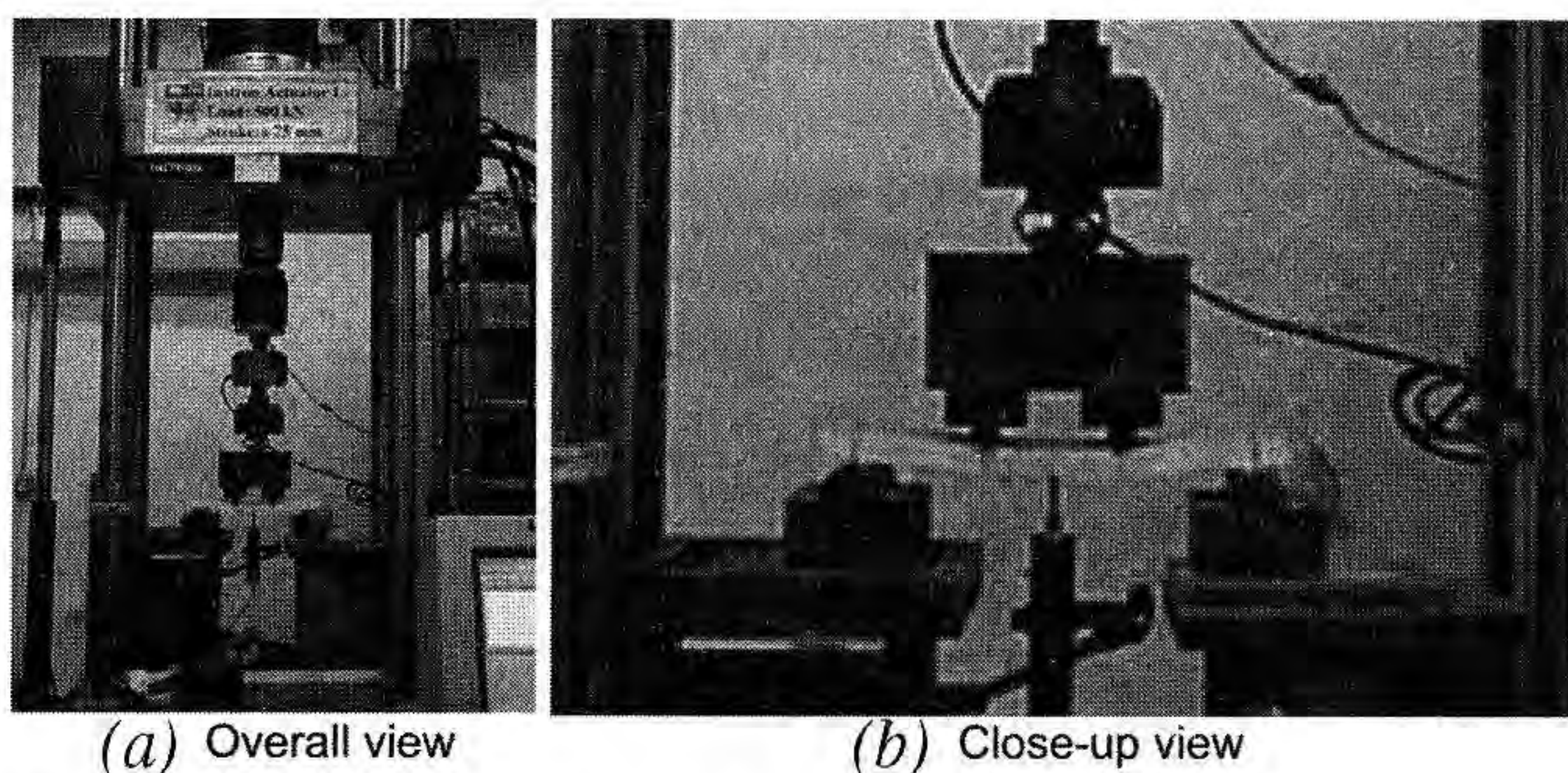


Fig. 4—View of setup for flexural strength test.

In the following discussion, maximum crack width, steel loss, and strength loss have been used separately as the required criteria for relative assessment of corrosion protection afforded by different protective systems considered in this study.

Cracking, crack development, and maximum crack width

Cracking induced by corrosion is due to the accumulation of corrosion products (rust) that exert bursting pressure to the surrounding concrete, and early cracking represents that the corrosion process is more severe. In this program, specimens left in a natural environment did not display any cracking. But those subjected to the accelerated corrosion regime exhibited cracking in as soon as 16 days of exposure, as can be seen in Table 3, despite the reinforcing system being distributed evenly and dispersed more uniformly than conventional reinforced concrete. This means that the accumulation of a corrosion product, rust, around the fine

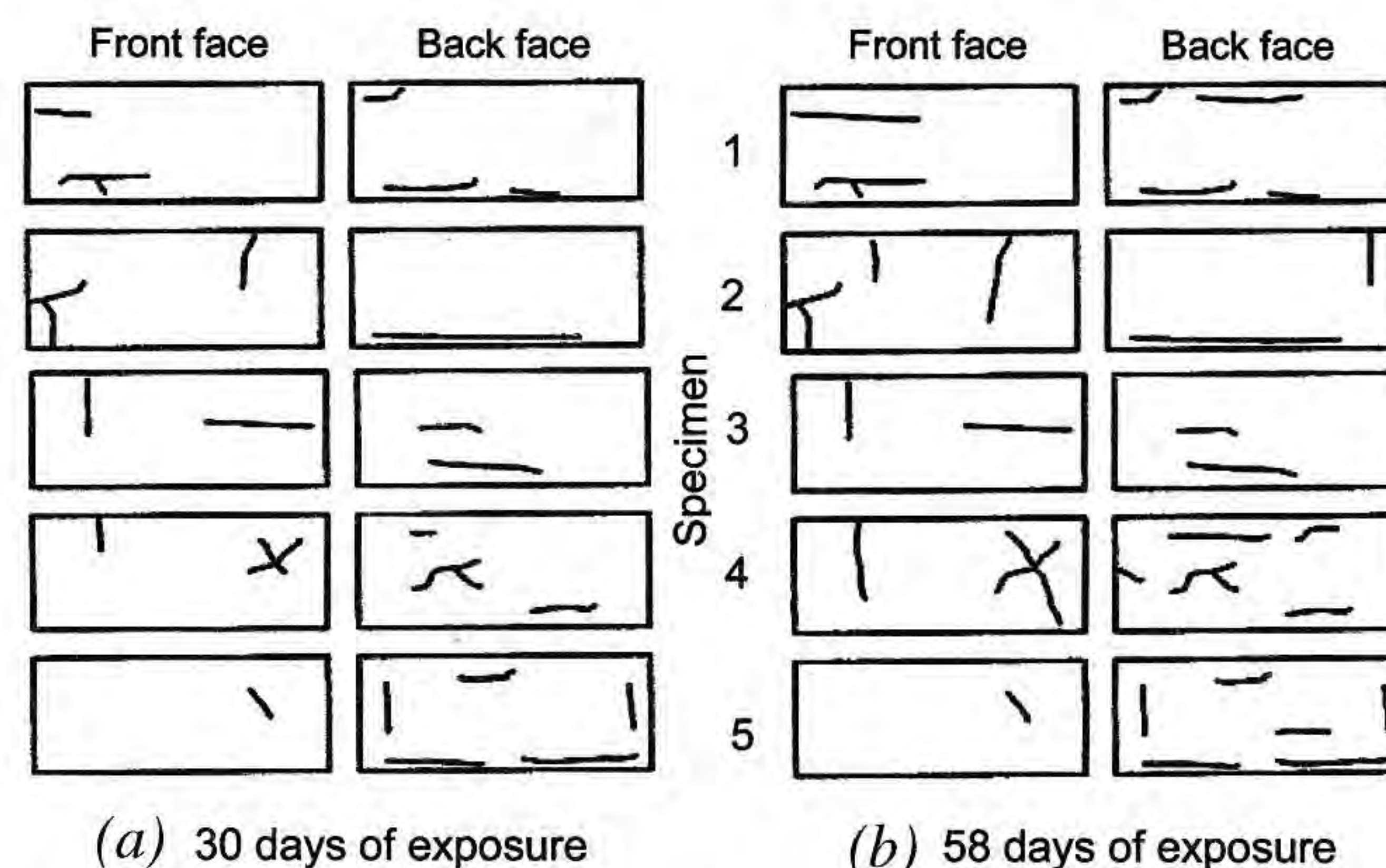


Fig. 5—Crack patterns and development of cracking in typical specimens.

Table 3—Principal test results

Parameter	Description	Specimen group	Mortar mixture	Onset of cracking, days	Maximum crack width, mm (in.)	Steel loss, %	Loss of strength, %
Type of steel	Galvanized	Control*	CM	25	0.2 (0.008)	7.9	57.0
	Stainless	SS	CM	16	0.3 (0.012)	2.6	41.3
Concrete cover, mm (in.)	3 (0.12)	CC-3	CM	16	0.25 (0.010)	9.2	63.2
	5 (0.20)	Control*	CM	25	0.2 (0.008)	7.9	57.0
	6 (0.24)	CC-6	CM	28	0.13 (0.005)	4.7	43.7
Surface coating	None	Control*	CM	25	0.2 (0.008)	7.9	57.0
	Sonoshield	SC	CM	35	0.02 (0.001)	3	38.2
w/c	0.35	w/c-0.35	w/c-0.35	28	0.07 (0.003)	8.4	51.9
	0.425	Control*	CM	25	0.2 (0.008)	7.9	57.0
	0.50	w/c-0.50	w/c-0.50	21	0.19 (0.007)	13.3	41.5
s/c	1.5	s/c-1.5	s/c-1.5	25	0.21 (0.008)	8.7	54.9
	2.0	Control*	CM	25	0.2 (0.008)	7.9	57.0
	2.5	s/c-2.5	s/c-2.5	28	0.10 (0.004)	16.6	69.7
Fly ash/cement	0%	Control*	CM	25	0.2 (0.008)	7.9	57.0
	25%	FA-25	FA-25	25	0.02 (0.001)	4.5	32.5
	50%	FA-50	FA-50	28	0.03 (0.001)	5.2	27.6
Silica fume/cement	0%	Control*	CM	25	0.2 (0.008)	7.9	57.0
	10%	SF-10	SF-10	None	0.00	0.9	14.7
Corrosion inhibitor	None	Control*	CM	25	0.2 (0.008)	7.9	57.0
	5 L/m ³	CI	CM+	16	0.32 (0.013)	2.2	29.4

*Same specimen group.

wires could generate bursting pressure sufficient to split the mortar cover. All specimens developed cracking except for the specimens in Group SF-10 that contained 10% silica fume in the mortar mixture.

Typical cracking patterns, sketched on the 30th and 58th days of exposure, are shown in Fig. 5. It has been found that the cracking that developed in various specimens did not follow a consistent pattern. The location of the initiation of cracking and the subsequent development of crack patterns are unique to each specimen, even for the specimens in the same group. Cracks, once formed, kept on propagating with continued exposure; new cracks were developed and the specimens got stained due to the release of corrosion products

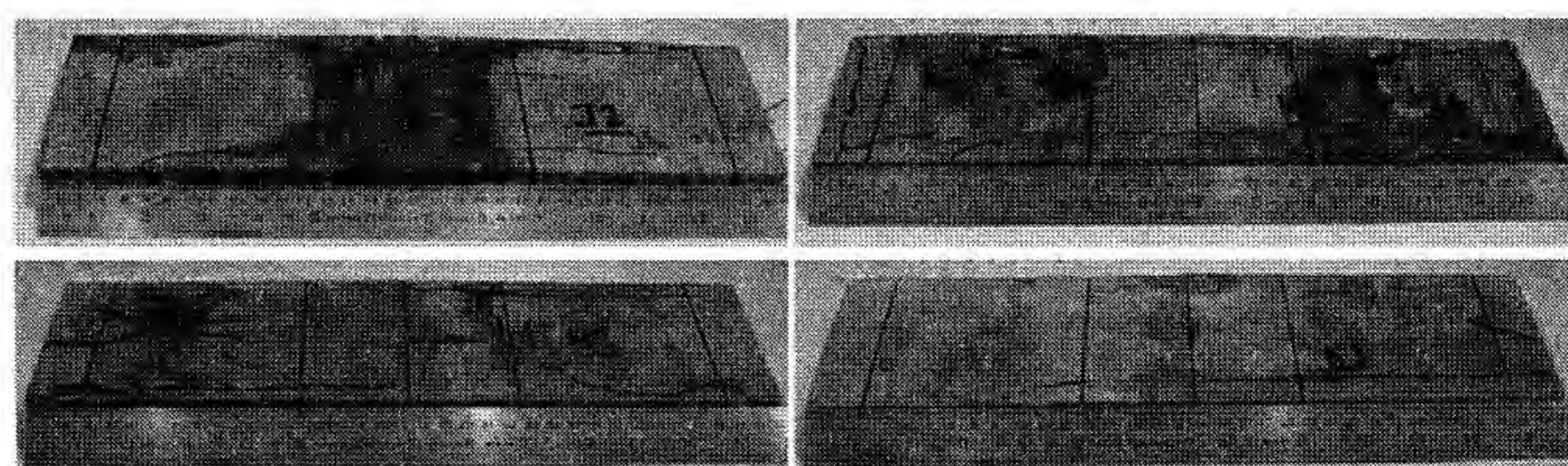


Fig. 6—Cracking and staining in typical specimens at end of accelerated corrosion.

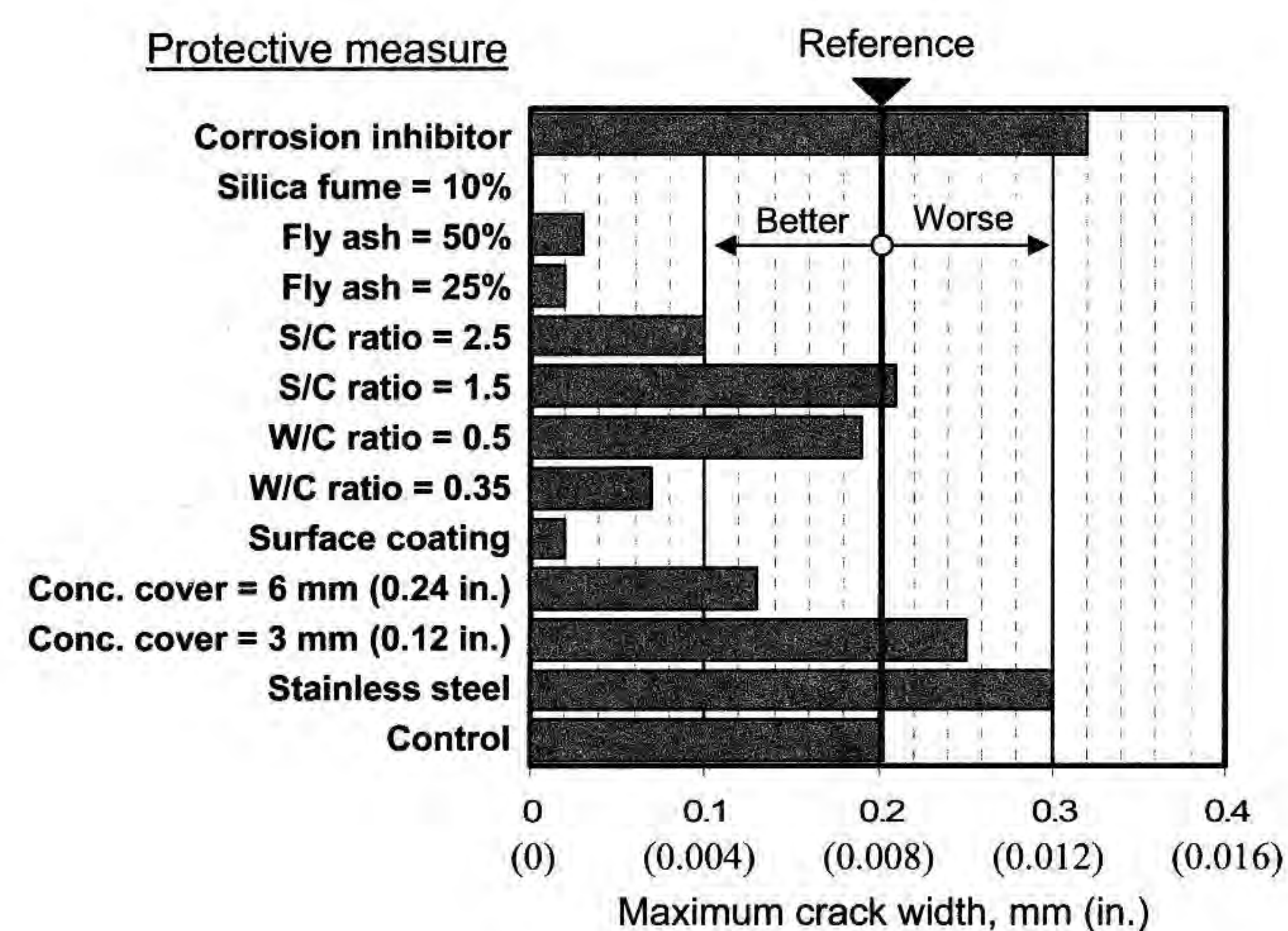


Fig. 7—Assessment of corrosion resistance using maximum crack width as criterion.

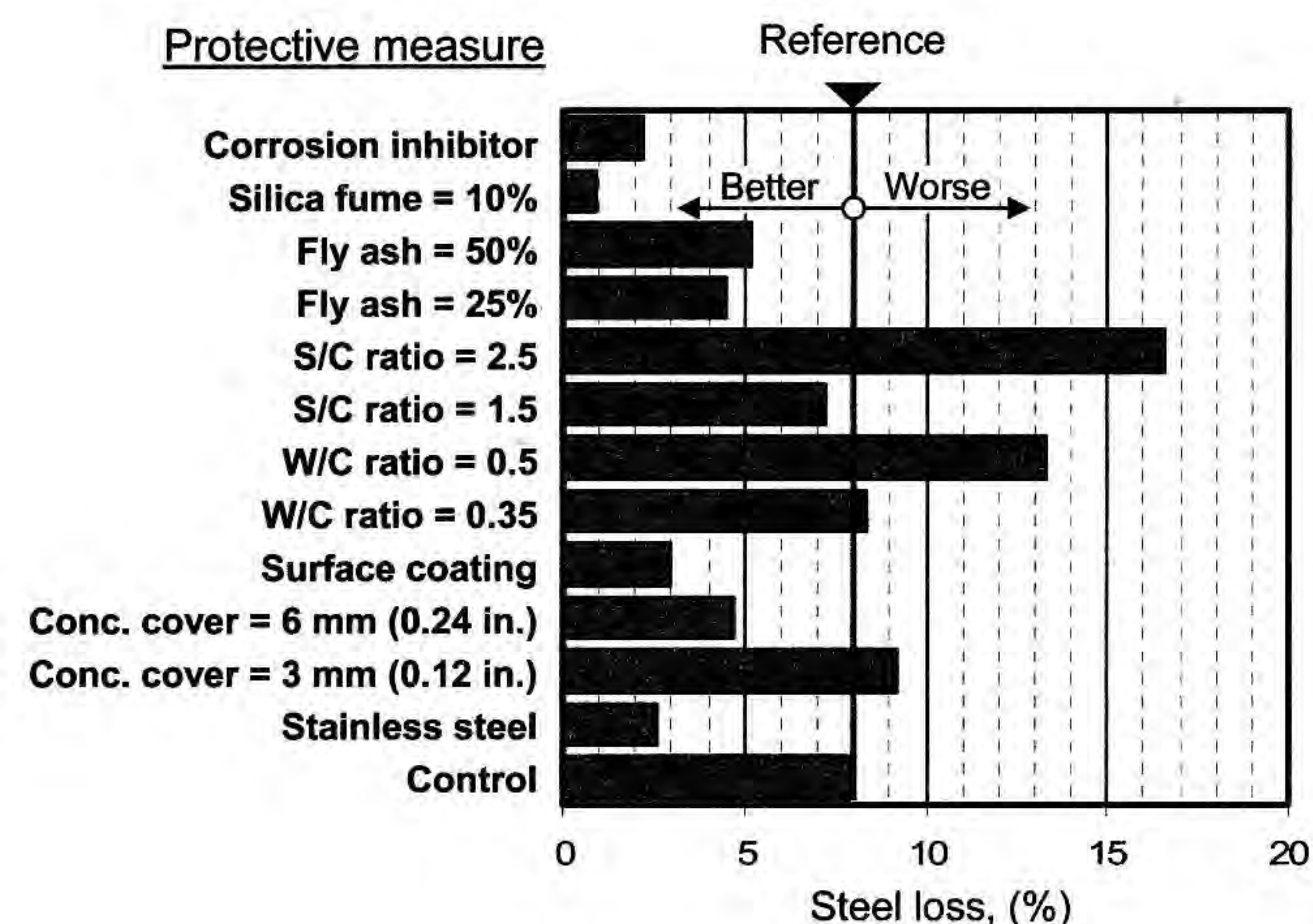


Fig. 8—Assessment of corrosion resistance using steel loss as criterion.

(refer to Fig. 6). In general, specimens that cracked early demonstrated larger maximum crack widths at the end of the corrosion regime.

The average maximum crack widths recorded for each group of specimens are plotted in the bar chart of Fig. 7 and compared with that of the control specimens (galvanized welded wire mesh as reinforcement, concrete cover equal to 5 mm [0.2 in.], w/c equal to 0.43, no admixture, and no surface coating). If this is taken as the criterion for the assessment of corrosion protection, then it may be clearly seen in Fig. 7 that using a lower w/c for the mortar mixture, a deeper concrete cover, incorporating mineral admixtures such as silica fume and fly ash in the mixture, or providing a suitable surface coating leads to considerable improvement in delaying the corrosion process—the most effective one being 10% silica fume followed by surface coating and 25% fly ash. Contrary to general expectation, use of corrosion inhibitors in the mortar mixture or employment of stainless steel reinforcement had demonstrated poorer resistance to corrosion with respect to maximum crack width.

Steel loss

In this study, the corrosion current was continuously monitored throughout the entire regime and the loss of steel as a consequence of corrosion was then indirectly estimated by using the well known Faraday's Law. According to this law, the current I , impressed during an electrochemical reaction, and the incremental steel loss Δ_w is related by

$$\Delta_w = \frac{MI t}{zF} \quad (1)$$

where Δ_w is the mass of steel consumed (g), M is the atomic weight of metal (56 g [0.123 lb] for Fe), I is the current (A), t equals time (seconds), z is the valency (2 for Fe), and $F = 96,500$ (A·s).

In using Faraday's Law, 100% current efficiency is assumed. This assumption implies that the current delivered to a specimen is entirely used up in oxidation of iron into ferrous ions and that oxidation of iron occurs by no other means. Heat losses, as well as formation of other independent cells, are ignored. Hence, Faraday's Law tends to overestimate the actual steel loss by approximately 180%.¹⁰ Such an estimate should, however, be acceptable for the assessment of relative performance of various protective systems, as used in this study.

The loss of steel, calculated for each specimen by using Eq. (1), was found to remain mostly within $\pm 20\%$ of the average of three specimens in a particular group. These average values are presented in Table 3 and plotted in the bar chart of Fig. 8 to facilitate comparison with the control specimens. It may be seen that, similar to the maximum crack width, using deeper concrete cover, incorporating mineral admixtures such as silica fume and fly ash in the mixture, or providing a suitable surface coating leads to a considerable reduction in steel loss; 10% silica fume offered the best protection. Unlike the excellent performance displayed by a low w/c of 0.35 with respect to maximum crack width, it only marginally equals the performance of the control specimens when this criterion is used. Also, it is interesting to note that, despite poorer performance of corrosion inhibitor and stainless steel reinforcement with regard to maximum crack width, they provided excellent corrosion protection when total steel loss was concerned.

Loss of strength

Deterioration or loss of strength as a consequence of reinforcement corrosion presents yet another means of indirectly assessing relative corrosion damage. In this study, five identical specimens were prepared for each group, two were kept under natural environment and the rest had gone through the accelerated corrosion regime. At the end of the desired period, all specimens were tested to failure in flexure to evaluate the changes in structural response, including the loss of strength due to corrosion.

Figure 9 shows the typical load-deflection response of two groups of specimens. It may be seen that the specimens that had gone through accelerated corrosion demonstrated not only strength loss, but also a loss in ductility. These specimens fractured suddenly into two parts through a major crack without displaying much deformation, though the

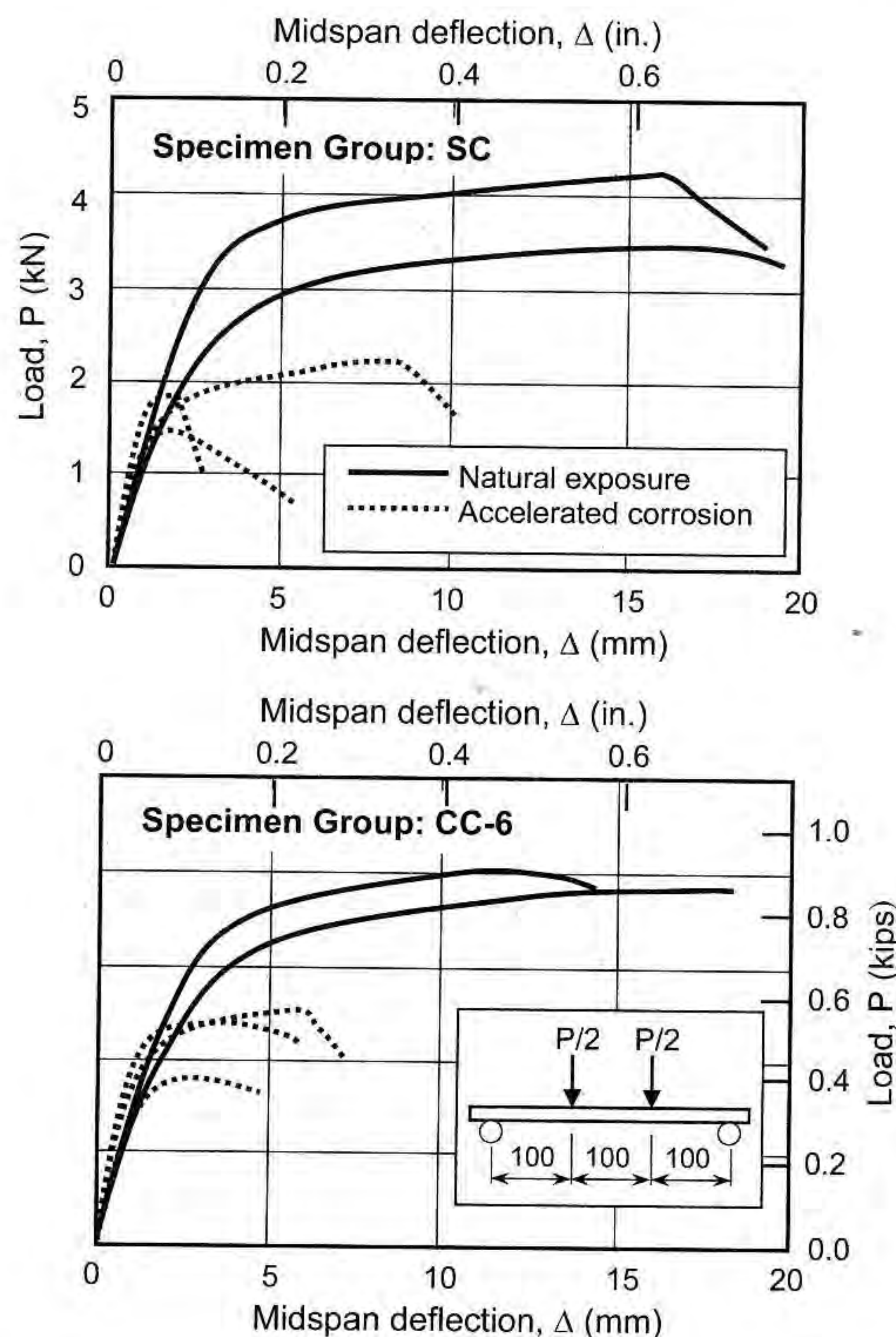


Fig. 9—Effects of accelerated corrosion on overall flexural response of typical specimens.

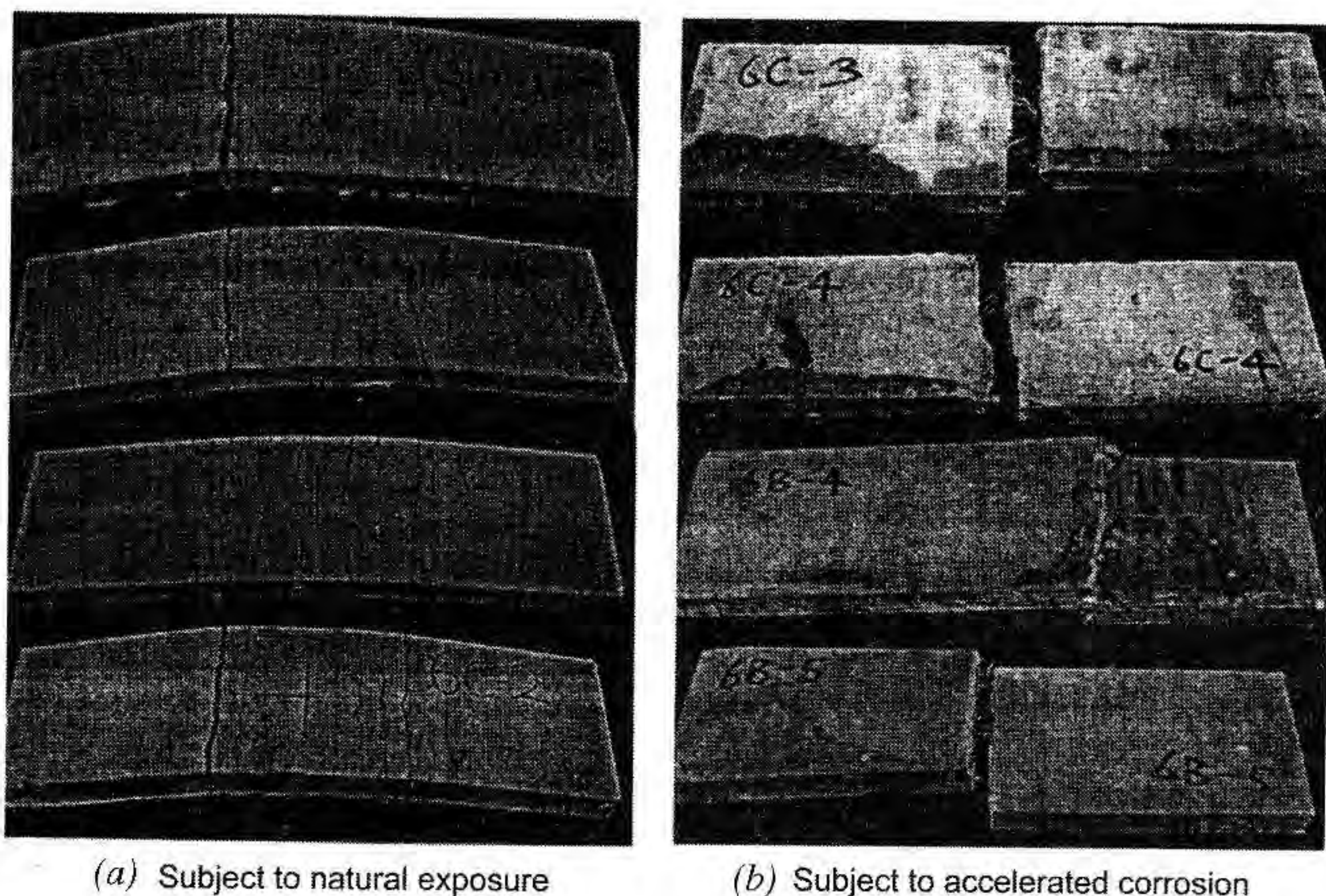


Fig. 10—Typical specimens after failure under flexural loading.

companion specimens kept under natural environment deformed quite considerably with the development of a well distributed crack pattern before failure. The brittle nature of failure of corroded specimens can also be noted in Fig. 10.

The values of strength loss calculated, on the basis of average experimental ultimate loads, for various groups of specimens are presented numerically in Table 3 and graphically in Fig. 11. Once more, the beneficial effects of using mineral admixtures, deeper concrete cover to reinforcement, and suitable surface coating in delaying the corrosion process are obvious; use of 10% silica fume providing the best protection yet again. Also, the use of a lower w/c , corrosion inhibitor, or stainless steel reinforcement led to a much better preservation of strength reflecting better performance than the assessment made using the maximum crack width criterion.

Overall assessment and recommendations

The preceding discussion dealt with the performance assessment of each protective system using the criteria of maximum crack width, steel loss, and strength loss separately. A careful examination of the numerical values of maximum crack width, steel loss, and strength loss with reference to the control specimens reveals that the level of protection afforded by a system is not consistent for all three assessment

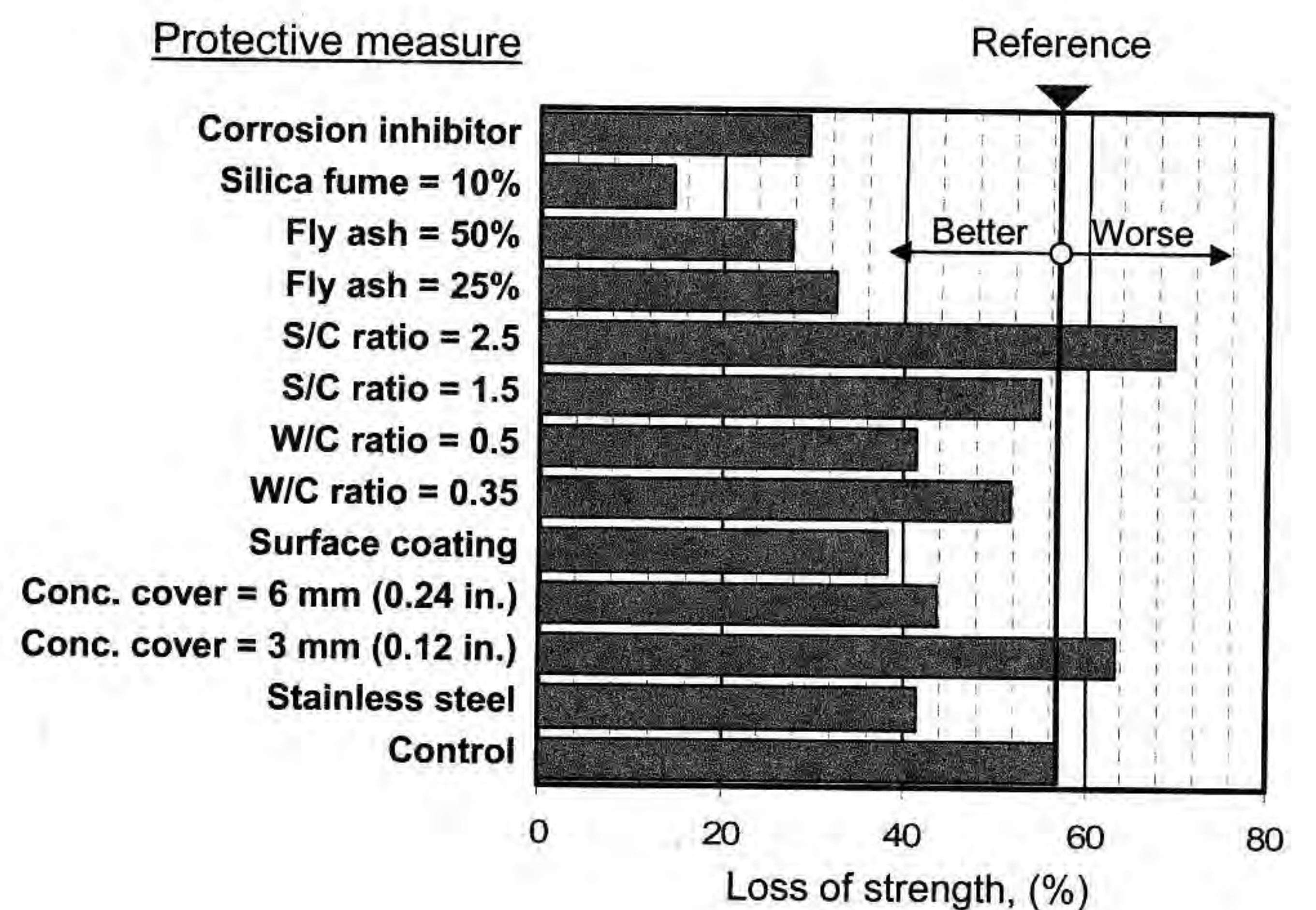


Fig. 11—Assessment of corrosion resistance using strength loss as criterion.

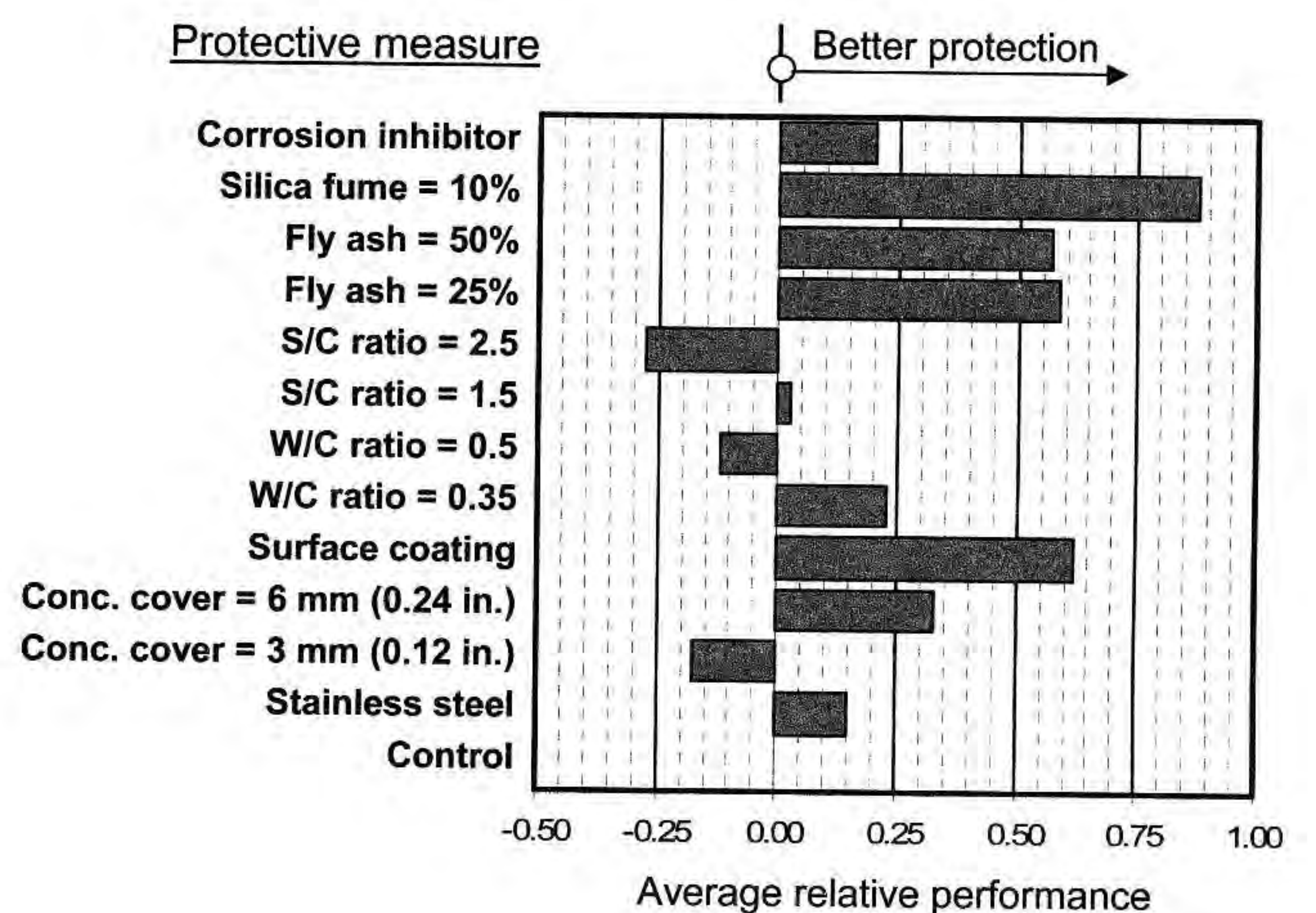


Fig. 12—Overall assessment of protective measure against reinforcement corrosion.

criteria used. To grade the protective system in terms of effectiveness in delaying the corrosion process, there is a need to make an overall assessment embracing all three assessment criteria.

In the present analysis, the relative performance of a protective system for a given assessment criterion has been evaluated by subtracting the value of the maximum crack width, steel loss, or strength loss, as appropriate from that of the control specimens and dividing this by the value of the control specimen. Mathematically, the relative performance (RP) demonstrated by a protective system may be expressed as

$$RP = \frac{(x)_{control} - (x)_{test}}{(x)_{control}} \quad (2)$$

where x represents the measured maximum width of cracks, percentage loss of steel, and percentage loss of strength for the assessment criteria of maximum crack width, steel loss, and strength loss, respectively, and the subscripts "control" and "test" denote the control specimens and test specimens representing a given protective system, respectively. Obviously, the value of RP is zero for the control (reference) specimen. Better performance is reflected by a larger number.

The three values, thus calculated for the three assessment criteria, were then averaged to reflect the overall performance relative to the control specimens. Plotted in Fig. 12, these values help to identify the effectiveness of different solo systems and grade them according to the relative overall performance. It may be seen that the best protection is provided when the mortar mixture contains 10% silica fume. This is followed by surface coating, 25% fly ash, 50% fly ash, and thicker cover in decreasing order of performance. These are followed by the use of a low w/c , corrosion inhibitor, and stainless steel.

Stainless steel and corrosion inhibitor are quite expensive components for the level of protection they provide to ferrocement, as reflected in this study. Instead, use of traditional galvanized steel may be combined with other cheaper and more effective means of corrosion protection for enhanced durability. From the results of this study, a hybrid protective system comprising silica fume, deeper concrete cover, lower w/c , and a suitable surface coating is recommended. If silica fume is not affordable or unavailable locally, the use of fly ash in moderate amounts should be considered. Although not covered in this study, the importance of adequate curing in enhancing corrosion durability of ferrocement should not be overlooked.¹¹ It should be noted herein that, whatever protective system is used, the long-term durability of a structure largely depends on how it is looked after subsequent to its construction. Once built, it should undergo regular inspection and maintenance, and this holds the key to prolonging the useful service life of a structure.

CONCLUSIONS

In this study, an attempt has been made to identify a suitable protective system for delaying or slowing down the deterioration process of ferrocement caused by reinforcement corrosion by conducting a series of accelerated corrosion

tests. The effectiveness of a measure has been evaluated by using maximum crack width, steel loss, and degradation of strength as the assessment criteria. From the results presented and discussed in this paper, the following conclusions may be drawn:

1. Despite containing more well distributed and evenly dispersed reinforcement elements in ferrocement compared with traditional reinforced concrete, accumulation of rust around fine wires resulted in the development of a bursting pressure sufficient to generate cracking;
2. The loss of steel as a consequence of corrosion leads to a reduction not only in strength but also in ductility and transforms ferrocement, an otherwise ductile material of outstanding quality, into a brittle one;
3. Among the measures investigated, incorporation of silica fume in the matrix consistently provided the best protection irrespective of the assessment criteria used;
4. Application of a suitable surface coating, use of deeper cover, and addition of fly ash also provide excellent protection to possible corrosion of steel reinforcement;
5. In ferrocement, replacement of fine galvanized wire mesh by an equivalent stainless steel is not warranted. The level of improvement demonstrated in this study by stainless steel may perhaps be accomplished by resorting to other cheaper means of corrosion protection; and
6. The hybrid protective system, as proposed herein by combining the three lines of defense is deemed to provide adequate protection against reinforcement corrosion, thus prolonging the service life of a ferrocement structure. It has been emphasized that, for enhanced durability, the need for adequate curing at the time of construction and the importance of regular inspection and maintenance should not be overlooked.

REFERENCES

1. ACI Committee 549, "Report on Ferrocement (ACI 549R-97)," American Concrete Institute, Farmington Hills, MI, 1997, 26 pp.
2. Naaman, A. E., *Ferrocement and Laminated Cementitious Composites*, Tehno Press, MI, 2000, 372 pp.
3. Mansur, M. A.; Paramasivam, P.; Wee, T. H.; and Lim, H. B., "Durability Of Ferrocement—A Case Study," *Journal of Ferrocement*, V. 26, No. 1, 1996, pp. 11-19.
4. Shah, S. P.; Lub, K. B.; and Ronzoni, E., "A Summary of Ferrocement Construction and A Survey of Its Durability (RILEM Committee 48-FC)," *Materials and Structures, Research and Testing*, V. 19, No. 112, RILEM, Paris, France, 1986, pp. 17-25.
5. International Ferrocement Society, "Ferrocement Model Code," Bangkok, Thailand, 2003, pp. 1.1-6.21.
6. Neville, A. M., *Properties of Concrete*, 4th Edition, John Wiley & Sons, Inc., New York, 1996, 844 pp.
7. Rosenburg, A.; Nansson, C. M.; and Andrade, C., "Mechanism of Corrosion of Steel in Concrete," *Material Science of Concrete*, 1989, pp. 285-313.
8. Yaleyne, H., and Ergun, M., "The Prediction of Corrosion Rates of Reinforcing Steels in Concrete," *Cement and Concrete Research*, V. 26, No. 10, 1996, pp. 1593-1599.
9. Lee, C., "Accelerated Corrosion and Repair of Reinforced Concrete Columns Using CFRP Sheets," MASC thesis, Department of Civil Engineering, University of Toronto, Toronto, ON, Canada, 1998, 106 pp.
10. Aiello, J., "The Effect of Mechanical Restraint and Mix Design on the Rate of Corrosion in Concrete," MEng thesis, Department of Civil Engineering, University of Toronto, Toronto, ON, Canada, 1996, 109 pp.
11. Nagataki, S.; Mansur, M. A.; and Ohga, H., "Carbonation of Mortar in Relation to Ferrocement Construction," *ACI Materials Journal*, V. 85, No. 1, Jan.-Feb. 1988, pp. 17-25.